THE JOURNAL OF BIOLOGICAL CHEMISTRY VOL. 283, NO. 50, pp. 34712–34719, December 12, 2008

The Tumor Marker Human Placental Protein 11 Is an Endoribonuclease*[S]

Received for publication, July 28, 2008, and in revised form, October 16, 2008 Published, JBC Papers in Press, October 20, 2008, DOI 10.1074/jbc.M805759200

Pietro Laneve[‡], Ubaldo Gioia[§1], Rino Ragno[¶], Fabio Altieri[‖], Carmen Di Franco[§], Tiziana Santini[§], Massimo Arceci[‡], Irene Bozzoni[‡§], and Elisa Caffarelli[‡2]**

*From the [‡]Istituto di Biologia e Patologia Molecolari, Consiglio Nazionale delle Ricerche, the [§]Dipartimento di Genetica e Biologia Molecolare, the [¶]Dipartimento di Chimica e Tecnologie del Farmaco, the [‖]Dipartimento di Biochimica, and the **Istituto Pasteur Fondazione Cenci-Bolognetti, "Sapienza" Università di Roma, Piazzale Aldo Moro 5, 00185 Rome, Italy*

Human PP11 (placental protein 11) was previously described as a serine protease specifically expressed in the syncytiotrophoblast and in numerous tumor tissues. Several PP11-like proteins were annotated in distantly related organisms, such as worms and mammals, suggesting their involvement in evolutionarily conserved processes. Based on sequence similarity, human PP11 was included in a protein family whose characterized members are XendoU, a *Xenopus laevis* endoribonuclease involved in small nucleolar RNA processing, and Nsp15, an endoribonuclease essential for coronavirus replication. Here we show that the bacterially expressed human PP11 displays RNA binding capability and cleaves single stranded RNA in a Mn^{2+}-dependent manner at uridylates, to produce molecules with 2′,3′-cyclic phosphate ends. These features, together with structural and mutagenesis analyses, which identified the potential active site residues, reveal striking parallels to the amphibian XendoU and assign a ribonuclease function to PP11. This newly discovered enzymatic activity places PP11-like proteins in a completely new perspective.

PP11 (placental protein 11) is one of the five glycoproteins (together with PP8, PP9, PP10, and PP12) that were first isolated from aqueous extracts of human term placentas in the 1980s. Unlike PP8 and PP9, which were found in relatively high concentrations in all tissues analyzed, PP10, PP11, and PP12 were supposed to be specific to the placentas, since they could not be detected in extracts of other human tissues (1, 2). Interestingly, it was shown that the placenta-specific proteins were also expressed in several tumor tissues; PP11 was detected in 66.7% of the analyzed mucinous cystadenocarcinomas and in 57.1% of serous cystadenocarcinomas tested, whereas it was not found in normal ovaries (3). Moreover, PP11 was also found in 47% of all breast cancers examined (4) and in 38% of all testicular and gastric cancers studied (5). These results suggested that this protein may be involved in carcinogenesis and, therefore, may represent a suitable molecular marker for tumor diagnosis.

A putative function for PP11 was proposed in 1990, when the cDNA was isolated from a placental cDNA library and the encoded protein was expressed in *Escherichia coli*; two different forms, a precursor of 45 kDa and a mature protein of 42 kDa, were produced. Employing a colorimetric assay on purified placental protein and on periplasmic and cytoplasmic fractions of extracts prepared from *E. coli*, containing the 42- and 45-kDa proteins, respectively, a putative serine protease activity was assigned to the placental and to the recombinant 42-kDa proteins (6). Another piece of information, which may contribute to the understanding of PP11 biological role, derives from its subcellular localization; PP11 was exclusively localized in the cytoplasm of syncytiotrophoblast (7). Since then, PP11 has not been subjected to further characterization, validating its protease activity and investigating its natural substrates.

Recently, PP11 has been identified as a member of the "XendoU family," a novel protein class including several enzymes that share a significant sequence homology with the founding member XendoU (8, 9). This enzyme is an amphibian endoribonuclease that participates in the biosynthesis of small nucleolar RNAs, a class of noncoding RNAs involved in ribosome biogenesis (10–12). Its viral homolog Nsp15, the second family member characterized, is an endoribonucleolytic activity considered as a major genetic marker of the Nidovirales order, including the coronavirus responsible for the severe acute respiratory syndrome (13, 14). Notably, even if the specific substrate of Nsp15 has not yet been identified, an essential role for this protein in virus replication and transcription was established (13, 14).

Within the XendoU family, PP11 is highly conserved both in vertebrates and in invertebrates (11). The finding that the human protein shares both a high sequence homology (38% identity and 55% similarity) and a predicted secondary structure with XendoU (9, 12) did not support its putative serine protease activity: accordingly, no canonical catalytic triad, typical of serine proteases, was found in homology modeling of PP11 (9). To delve into its function, we expressed a recombinant histidine-tagged PP11 (His-PP11) and employed the purified protein to investigate several aspects concerning its enzymatic activity, biochemical properties, and cellular localization. Here we show that PP11 has RNA binding activity, whereas it

* This work was supported in part by grants from the 6th Framework Programme of the European Commission (SIROCCO Project, LSHG-CT-2006-037900), the ESF project "NuRNASu", PRIN and Centro di Eccellenza BEMM, Associazione Italiana Ricerca sul Cancro (AIRC) and AIRC-Rome Oncogenomic Center. The costs of publication of this article were defrayed in part by the payment of page charges. This article must therefore be hereby marked "*advertisement*" in accordance with 18 U.S.C. Section 1734 solely to indicate this fact.

[S] The on-line version of this article (available at http://www.jbc.org) contains supplemental Figs. 1–9.

[1] Supported by a fellowship from AIRC/FIRC.

[2] To whom correspondence should be addressed. Tel.: 390649912201; Fax: 390649912500; E-mail: elisa.caffarelli@uniroma1.it.

does not display the predicted serine protease function; it proved to be an endoribonuclease sharing the main biochemical features (*i.e.* ion requirement, cleavage site specificity, and released products) with the RNases belonging to the same family. Furthermore, homology modeling in parallel with site-directed mutagenesis allowed us to determine the residues crucial for its catalytic activity.

EXPERIMENTAL PROCEDURES

Proteolytic Activity Assay—Proteolytic activity was determined by a chromogenic assay with Chromozyme TH (Roche Applied Science), following the variation of absorbance at 405 nm. Other hydrolase activities were measured using 2 mM *p*-nitrophenyl acetate (15) and 5 mM glycine *p*-nitroanilide as substrates, both in 0.1 M Tris-HCl, pH 8.0, and following the variation of absorbance at 405 and 435 nm, respectively. For each assay, aliquots of protein, containing 1–20 μg, were employed, and the reactions were carried out at 37 °C in the presence or absence of different cations. Thrombin from bovine plasma (Roche Applied Science) and rabbit liver esterase (Sigma) were used as reference activity.

Homology Modeling and Docking—The PP11 sequence (UniProtKB/Swiss-Prot entry P21128) was retrieved from the ExPASy (Expert Protein Analysis System) World Wide Web server and then was submitted to the HHpred and the Swiss-Model homology model World Wide Web servers. Both of the servers identified the XendoU structure as the most suitable to generate the PP11 three-dimensional model; therefore, it was selected as the three-dimensional template (Protein Data Bank code 2c1w). The generation of the PP11 three-dimensional models was run using the default options in both of the homology model servers. Due to steric hindrance that is generated upon hydrogen addition, the two models were geometrically optimized using the AMBER 8 molecular modeling suite. To this the HHpred and the Swiss-Model models in turn were solvated (SOLVATEOCT command) in a box extending 10 Å with 7977 (Swiss-Model) or 12151 (HHpred) water molecules (TIP3 model) and neutralized with eight Na^+ ions. The solvated complex was then refined by minimization (5000 iterations) using the SANDER module of AMBER. For the graphical inspection of the minimized models and image production, Chimera 1.2470 (University of California, San Francisco) was used. The secondary structure of the oligoribonucleotide P1 (GGAACGUAUCCUUUGGGAG) was calculated with the mfold program (available on the World Wide Web) with the default setting. Next, a limited version of the Mc-Sym program (available on the World Wide Web) was run to generate the three-dimensional models of the predicted stem-loop structural motifs present in two mfold-suggested P1 secondary structures (RNA1 and RNA2). The docking studies were performed by means of the Autodock 3.0.5 program using a grid spacing of 0.375 Å and 80 × 80 × 80 points that embraced almost half of the protein. The grid was centered on the mass center of the corresponding XendoU experimental bound phosphate. The Genetic Algorithm Local Search method was adopted using the default setting, except that the maximum number of energy evaluations was increased from 250,000 to 2,500,000. Autodock generated 100 possible binding conformations for each molecule that were clustered using a tolerance of 2.0 Å. The AutoDockTool graphical interface was used to prepare the enzyme PDBQS file. The protein atom charges as calculated during the complex minimization were retained for the docking calculations. In the docking of the two RNA substrates, no bonds were allowed to rotate.

The GU and UU dinucleotides were built, starting from ASCII text, using the stand alone version of PRODRG, in conjunction with the GROMACS suite. The dockings of the UU and GU dinucleotides were conducted allowing rotation of all rotatable bonds.

Oligonucleotides—The following DNA oligonucleotides, purchased from Sigma, were used for cloning the different constructs: START, 5′-TCCCCCGGGTGAGGACCACAAAGAGTCAGAG-3′; STOP, 5′-CCCAAGCTTTTAGGTGGAAGACACTATGTAGGC-3′; E243fw, 5′-CAACATGTCTTCTCAGGTGAGG-3′; E243rev, 5′-AAAGCCACTCGAGTCCCC-3′; H244fw, 5′-GTCTTCTCAGGTGAGGTAAAAAAAGG-3′; H244rev, 5′-AGCTTCAAAGCCACTCGAGTCCC-3′; E249fw, 5′-CAGGTAAAAAAAGGCAAGGTTACTGGC-3′; E249rev, 5′-ACCTGAGAAGACATGTTCAAAGCC-3′; H259fw, 5′-GCTAACTGGATCCGCTTCTACC-3′; H259rev, 5′-GAAGCCAGTAACCTTGCC-3′; K302fw, 5′-GCGGAAGTGGGCTCTGCTTTCATCG-3′; K302rev, 5′-ATAGTAGCCGTCCCAGTTGAACTGC-3′.

Cloning and Expression of His-PP11 and Its Mutant Derivatives—PP11 open reading frame was amplified from I.M.A.G.E. cDNA 8 Digit Clone 30915175 (MRC Geneservice, Cambridge, UK) by standard PCR, employing the synthetic oligonucleotides START and STOP and cloned downstream of the His_6 tag coding sequence in the pQE30 expression vector (r-hPP11).

The plasmids expressing His-PP11 mutant derivatives were realized by inverse PCR on an r-hPP11 construct with the oligonucleotides indicated in parentheses: E243Q (E243fw, E243rev), H244A (H244fw, H244rev), E249Q (E249fw, E249rev), H259A (H259fw, H259rev), and K302A (K302fw, K302rev).

All recombinant proteins were expressed in the *E. coli* M15 (pREP4) strain and purified by affinity chromatography as already described for XendoU (12, 16).

In Vitro RNA Transcription, Binding, and Processing Reactions—The U16-containing precursor (mini 003 RNA) template was utilized for *in vitro* transcription according to Melton *et al.* (17) and employed in binding assays (12).

All of the oligoribonucleotide substrates were 5′-end-labeled with [γ-^{32}P]ATP (PerkinElmer Life Sciences) and incubated with different amounts of His-PP11 (wild type or mutant versions), using conditions described by Laneve *et al.* (11). Processing products were analyzed on 20% polyacrylamide, 7 M urea gels.

Double-stranded RNAs were obtained by denaturing labeled P2 oligonucleotide and incubating it with its cold counterpart in a molar ratio of 1:3 for 1 h at 37 °C in the processing buffer (5 mM $MnCl_2$, 50 mM NaCl, 25 mM Hepes, pH 7.5, 1 mM dithiothreitol, 20 units of RNase inhibitor (Amersham Biosciences)). Proper formation of double-stranded RNA was verified on nondenaturing gels. The nucleotide RNA ladder was obtained by

incubation of labeled oligonucleotides in 500 mM $NaHCO_3$ at 90 °C for 20 min.

Analysis of 3′ Termini—Gel-purified 5′-terminal cleavage product (derived by cleavage at the UU ↓ U stretch of P1 oligonucleotide) was incubated in 30 mM Tris, pH 8.0, 15 mM $MgCl_2$, and T4 polynucleotide kinase (New England Biolabs, Ipswich, MA) for 45 min at 37 °C to remove the 2′,3′-cyclic phosphate (18). As a negative control, RNA was treated with the indicated kinase buffer alone or with alkaline phosphatase (Roche Applied Science). After extraction and labeling in the presence of 5′-[^{32}P]cytidine 3′,5′-bisphosphate (PerkinElmer Life Science) and T4 RNA ligase (New England Biolabs) for 5 h at 16 °C, RNA was analyzed on 20% polyacrylamide, 7 M urea gel.

Purification of Anti-His-PP11 Antibodies—Anti-His-PP11 serum was obtained by immunization of rabbits (Primm, Milano, Italy) with the purified recombinant protein. Specific antibodies were purified by affinity chromatography using recombinant His-PP11 immobilized onto Affi-gel 10 (Bio-Rad). IgGs were eluted with 0.1 M glycine, pH 3, neutralized with phosphate buffer, pH 8, and utilized in immunofluorescence and Western blot experiments.

Processing of Placental Samples and BeWo Cells for Immunofluorescence—Normal term placentas were obtained with local research and ethics committee approval. Small fragments were immediately excised at random sites, briefly rinsed in phosphate-buffered saline to remove blood excess, and fixed in 4% buffered paraformaldehyde for 4 h. Samples were then infused in 12–18% sucrose in phosphate-buffered saline as cryoprotectant prior to liquid nitrogen freezing in OCT compound (Sakura Finetek Europe, Zoeterwoude, Netherlands). 6-μm cryosections were cut, mounted on SuperFrost-Plus glass slides (Menzel-Glaser, Brauschweig, Germany), air-dried, and then treated with 1 M glycine for 20 min and with 5% donkey serum, 5% bovine serum albumin for 2 h. Purified anti-His-PP11 antibodies were used at 1:300 dilution (overnight incubation at 4 °C) and revealed with 1:300 Alexa Fluor 594 donkey anti-rabbit secondary antibodies (Molecular Probes, Inc., Eugene, OR). The specificity of immunolabeling was verified in control samples prepared with the primary antibody omitted. The sections were counterstained with 1.5 mg/ml 4′,6-diamidino-2-phenylindole in Vectashield Mounting Medium (Vector Laboratories, Inc., Burlingame, CA) and analyzed in a Zeiss microscope (Carl Zeiss MicroImaging, Inc., Thornwood, NY) equipped with epifluorescence. BeWo choriocarcinoma cells (CCL-98; American Type Culture Collection, Manassas, VA) were maintained at 37 °C, under 5% CO_2, in Dulbecco's modified Eagle's medium/F-12 + GLUTAMAX^{TM} 1:1 (Invitrogen) supplemented with 10% fetal bovine serum, 100 units/ml penicillin, and 100 μg/ml streptomycin. For immunofluorescent studies, cells were grown on glass coverslips to confluence, rinsed twice with phosphate-buffered saline, and fixed for 15 min at 4 °C in freshly prepared formaldehyde (10%). The cells were processed for immunostaining as previously described for placental cryosections.

Western Blot Analysis—Small placental fragments, of about 300 mg, were directly frozen in liquid nitrogen. For protein extract preparation, the samples were thawed out, rinsed with phosphate-buffered saline, and homogenized in 1 ml of lysis buffer (10 mM Tris-HCl, pH 7.4, 100 mM EDTA, pH 8, 100 mM NaCl, 0.1% SDS) with Ultra-Turrax for 15–20 s on ice and incubated at 4 °C for 20 min. After centrifugation at 3000 relative centrifuge force at 4 °C for 10 min, the supernatant was stored at −20 °C. Extracts from BeWo cells were collected in radioimmune precipitation buffer. The extracts were fractionated onto NuPAGE 10% polyacrylamide gel (Invitrogen), blotted onto Protran nitrocellulose membrane (PerkinElmer Life Sciences), and reacted overnight with purified anti-His-PP11 antibodies (1:2500 in TBS, 1% Tween 20).

Bioinformatic Analysis—RNA secondary structures were predicted by the RNA mfold version 3.2 Web server (19). Structures with the lowest initial ΔG were selected. Histograms were generated by densitometric analyses performed employing ImageQuant TL version 2005 software (Amersham Biosciences).

The apparent K_d (K'_d) was calculated according to the equation, $K'_d = [\text{protein}_{\text{free}}] \times [\text{RNA}_{\text{free}}]/[\text{protein-RNA}]$ (20), and binding curves were best fit with Sigma Plot 10 using a sigmoidal dose-response curve.

RESULTS

PP11 Has No Detectable Serine Protease Activity—PP11 was previously isolated, thanks to its high levels of expression in the syncytiotrophoblast. We cloned a full-length PP11 cDNA fused to a His tag and purified the expressed 42-kDa protein in *E. coli* (His-PP11). In parallel, antibodies against the recombinant protein were generated, purified by affinity chromatography, tested on placental and BeWo cell protein extracts, and employed for immunofluorescence studies. These analyses indicated that the antibodies specifically recognized the His-PP11 protein as well as the two forms of the placental protein and confirmed the reported abundant expression of PP11 in syncytiotrophoblast (7) (supplemental Fig. 1).

Our previous PP11 homology modeling did not reveal any evidence for a catalytic triad that could account for its putative serine protease activity; the residues His^{162}, Ser^{157}, and Glu^{161} (or Asp^{156}) tend to cluster, but their stereochemistry does not conform to the canonical triad (9).

To unequivocally establish PP11 enzymatic activity as a protease and/or as esterase, the recombinant protein was employed in the amidolytic assay described by Grundmann *et al.* (6). The level of protease activity was undetectable by chromogenic assay on Chromozyme TH at all of the protein concentrations tested (Fig. 1). Supporting this result, no amidase activity was observed using glycine *p*-nitroanilide as substrate (not shown). A very low hydrolytic activity (less than 0.002 μmol min^{-1} mg^{-1}) was observed toward *p*-nitrophenyl acetate, indicating its preferential esterase activity (Fig. 1).

PP11 Homology Modeling—The sequence and secondary structure conservation of PP11 with XendoU endoribonuclease suggests an RNase activity for the human protein (9, 12).

To support this prediction, we performed a homology-modeling analysis on PP11, based on the XendoU crystallographic structure (9). Two three-dimensional models were automatically generated, employing two of the most widely used publicly available homology model Web servers, namely the Swiss-Model (21) and the HHpred (22). Both of the homology model

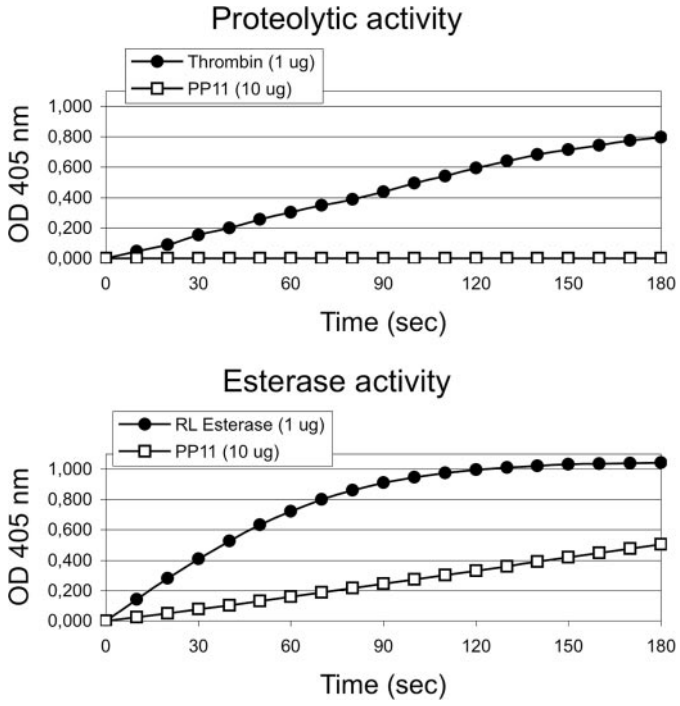

FIGURE 1. **Analysis of PP11 hydrolytic activities by chromogenic assay.** Proteolytic (*top*) and esterase (*bottom*) activities were determined by a chromogenic assay, using 1.25 mg/ml Chromozyme TH and 2 mM *p*-nitrophenyl acetate as substrates, respectively, and following the change in absorbance at 405 nm. The same amount of PP11 (10 μg) was tested in each assay. Thrombin from bovine plasma (1 μg) and rabbit liver esterase (*RL Esterase*; 1 μg) were used as reference activity.

servers identified the experimental three-dimensional structure of XendoU (Protein Data Bank code 2c1w) as the most appropriate template, with an identity sequence score of about 40%. The two homology models were quite superimposable (root mean square deviation = 0.532 over 168 residue pairs), except for a flap region, located between Gly^{248} and Asn^{260} (corresponding to Gly^{166}–Asn^{179} in XendoU) that is endowed with a certain flexibility. Inspection of the two models in comparison with the experimental three-dimensional structure of the template highlighted that the HHpred-derived PP11 model conserved the flap region in an open position, whereas the Swiss-model PP11 structure displayed a closed switched flap (Fig. 2, *a* and *b*, and supplemental Fig. 2).

In XendoU, the flap is kept opened by a hydrogen bonding net established between the side chains of Glu^{167}, Gln^{172}, and Lys^{220} (supplemental Fig. 3); such a flap region was detected to accommodate a phosphate group in XendoU experimental structure, suggesting this as the putative RNA binding site (9). In the modeled PP11, only the Glu^{249} residue, corresponding to the XendoU-Glu^{167} residue, is conserved, whereas counterparts of XendoU-Gln^{172} and -Lys^{220} change to Lys^{254} and Asp^{298}, respectively; as a consequence, the absence of the hydrogen bonding network could explain the enhanced flexibility of the PP11 Gly^{248}-Asn^{260} loop (supplemental Figs. 3 and 4). These modeling data allow us to speculate that the HHpred structural model represents the active state of the PP11 enzyme in which a putative RNA-binding domain can be recognized. We employed this structural model for further inspection of the possible enzyme/substrate interactions.

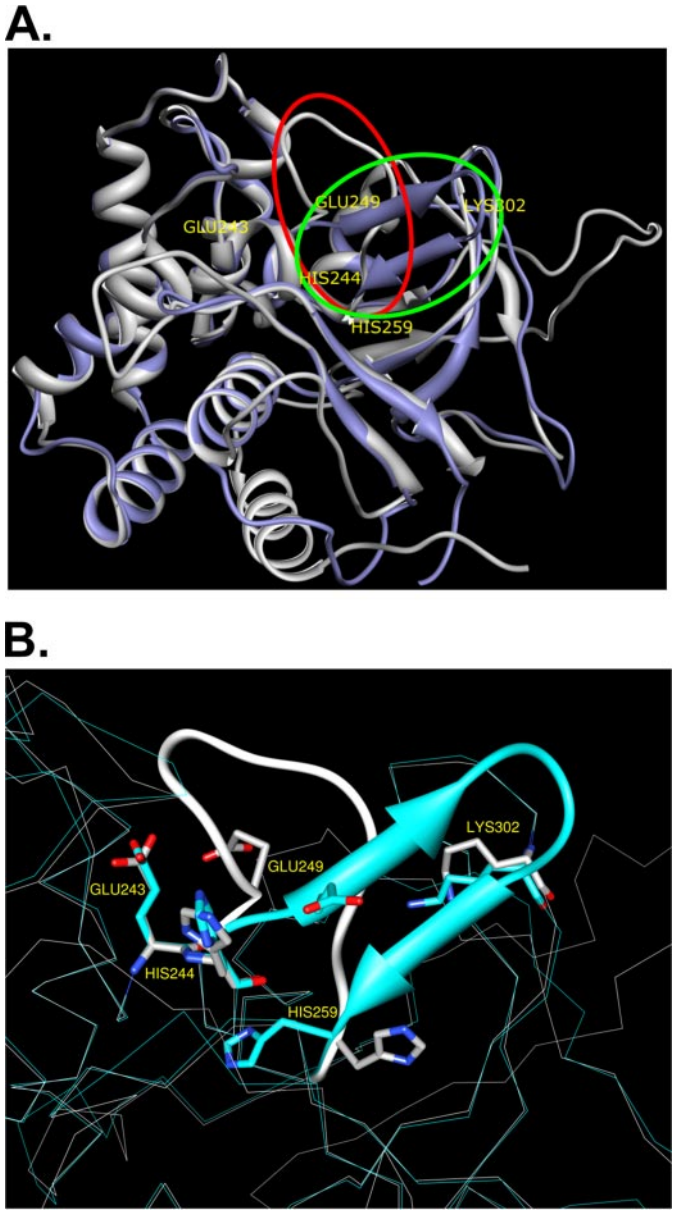

FIGURE 2. *A*, the HHpred-generated (*white*) and SwissModel-generated (*purple*) PP11 homology models. Mutated residues are depicted in *yellow*. The flexible flap is also highlighted with a *red circle* (open form) and *green circle* (*closed form*). *B*, the arrangement of PP11 catalytic residues and the positions of the polypeptide flexible flap segment (*cyan*, open form; *white*, closed form) are shown.

PP11 Interacts with RNA—The ability of the protein to interact with a RNA substrate was tested by *in vitro* binding assays. For this purpose, increased concentrations of His-PP11 were incubated with a fixed amount of ^{32}P-labeled mini 003 RNA that represents a short version of the XendoU natural substrate (12); we chose this molecule, since it displays the appropriate length, allowing the formation of stable RNA-protein complexes. The assembled complex was visualized by an electrophoretic mobility shift assay (Fig. 3*A*). In order to exclude the possibility that the His tag contributed to the RNA binding activity of PP11, a control binding experiment with an unrelated His tag fusion protein (acetyl-CoA synthetase) with no reported affinity for nucleic acids was performed. Only a very

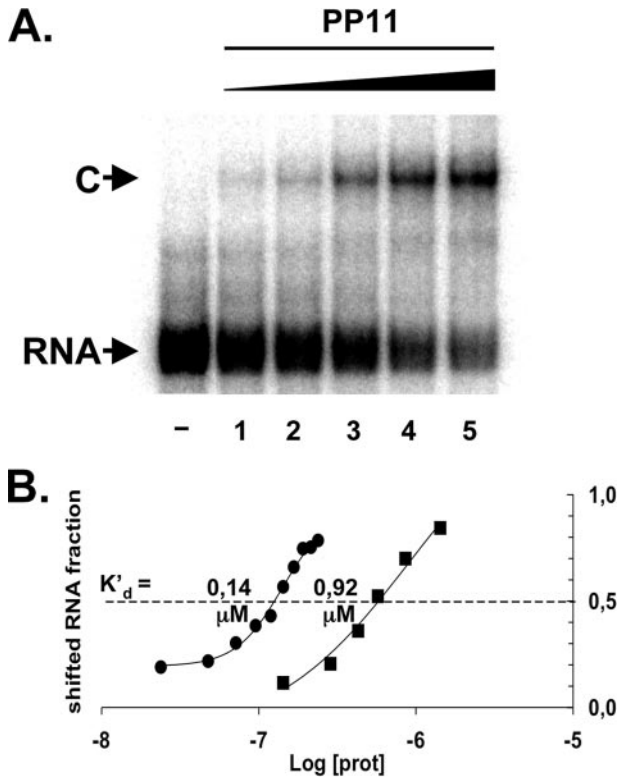

FIGURE 3. **Characterization of RNA binding activity of His-PP11.** *A*, 2 fmol of ^{32}P-labeled mini 003 RNA (*lane* −) were incubated with increasing amounts of His-PP11, 10 ng (*lane 1*), 20 ng (*lane 2*), 40 ng (*lane 3*), 60 ng (*lane 4*), and 80 ng (*lane 5*). The positions of free RNA (*RNA*) and RNA-protein complex (*C*) are indicated on the *left*. *B*, the fraction of shifted RNA substrate was reported *versus* the logarithm of XendoU (■) or PP11 (●) concentration. The inflection point *abscissa* of the fitted binding curve represents the protein apparent dissociation constant (K'_d).

minor nonspecific interaction was detected, summing up to no more than 2% of input RNA (supplemental Fig. 5).

The substrate affinity of PP11 and XendoU toward RNA was determined by measuring the apparent dissociation constant (K'_d). The estimated K'_d was equal to 140 nM for PP11 and 920 nM for XendoU, suggesting a higher RNA affinity for the human protein compared with the *Xenopus* enzyme (Fig. 3*B*).

RNA-protein interaction was further investigated through docking experiments, conducted by means of the Autodock program, (23), using the HHpred PP11 modeled structure. For such an experiment, we employed the sequence corresponding to the oligoribonucleotide P1 (GGAACGUAUCCUUUGGGAG) that contains a natural cleavage site of XendoU (11).

At first, two secondary structures of the oligoribonucleotide (supplemental Fig. 6) were generated, as suggested by the mfold program (19). The predicted stem-loop structural motifs present in both secondary structures were selected to produce RNA1 (GAACGUAU; supplemental Fig. 6, *left*) and RNA2 (CCUUUGGG; supplemental Fig. 6, *right*) three-dimensional models by the Mc-Sym program (24).

The Autodock-suggested RNA1-PP11 and RNA2-PP11 complexes (supplemental Fig. 7), although not overlapping each other, are relatively near to the flexible flap and close to the phosphate residue experimentally found in the XendoU structure (9). These results suggest that the PP11 Gly^{248}–Asn^{260} loop region is involved in RNA binding.

PP11 Has an Endoribonuclease Activity—To investigate the RNase activity of PP11, a collection of synthetic oligoribonucleotides was employed. All of them derived from P1, the oligonucleotide containing the UUU upstream distal cleavage site of XendoU; they are P2, P3, and P4, in which the UUU stretch is substituted by UU, UCU, and UGU sequences, respectively (see Fig. 4) (11). These molecules represent suitable substrates for testing both the ribonucleolytic activity and the sequence specificity of the enzyme.

The processing assay consisted in the incubation of the affinity-purified His-PP11 with ^{32}P-labeled oligoribonucleotides under the conditions already set up for XendoU activity (11). The reaction was carried out in the presence of manganese both at 24 °C, the temperature utilized for XendoU activity assay, and at 37 °C; since no differences were detected (not shown), all of the following assays were performed at 24 °C. Fig. 4 shows that His-PP11 cleavages occur 5′ of uridylates. The UU and GU sites (marked by *long arrows* in Fig. 4, *bottom*) are more efficiently cleaved than CU and AU sites (marked by *short arrows*). Nevertheless, this seems not to be a rigid rule, since UA and UC (marked by *arrowheads*) are also cleaved with a 12-fold lower efficiency, thus representing minor cleavage sites. Interestingly, all of the cleavage sites map in a putative single-stranded RNA structure, as predicted by the mfold program (Fig. 4, *bottom*). As a proof of concept, we experimentally demonstrated that the enzyme is unable to process double-stranded RNA (Fig. 4, *lane dsRNA*). In addition, using ^{32}P-labeled deoxyoligonucleotides, cleavage activity on DNA substrates was excluded as well (not shown).

Processing experiments were also performed in the presence of increasing substrate concentration. The results show that PP11 displays a saturable activity, with saturation occurring at comparable substrate/enzyme concentration (supplemental Fig. 8).

Docking experiments were extended to the GU and UU preferred cleavage dinucleotides; both of them were located in the corresponding XendoU phosphate binding region (9) (supplemental Fig. 9). The different orientation of the two dinucleotides may reflect the above reported enzyme binding site flexibility.

His-PP11 activity was further investigated by analyzing the ion dependence of cleavage; Fig. 5*A* shows that only Mn^{2+} ions trigger the RNase activity, whereas all the other examined ions (Mg^{2+}, Cd^{2+}, Co^{2+}, Cu^{2+}, Ni^{2+}, Zn^{2+}, and Pb^{2+}) were not effective.

Finally, the chemistry of His-PP11 cleavage was determined by analyzing the nature of the 3′ termini in the cleaved products. For this purpose, the major "e" product, generated by His-PP11 cleavage on P1 oligoribonucleotide, was gel-purified and ligated to 5′-[^{32}P]pCp directly or after alkaline phosphatase or kinase treatment. The first enzyme removes the linear phosphate group, whereas the second one specifically removes the 2′,3′-cyclic phosphate (18). As shown in Fig. 5*B*, the His-PP11 cleavage product is labeled only after kinase treatment (*lane 2*, "*e*" *molecule*), indicating that the 3′-end of the cleavage product carries a 2′,3′-cyclic phosphate. As control, the full-length P1 oligonucleotide underwent the same treatments (Fig. 5*B*, *lanes P1*).

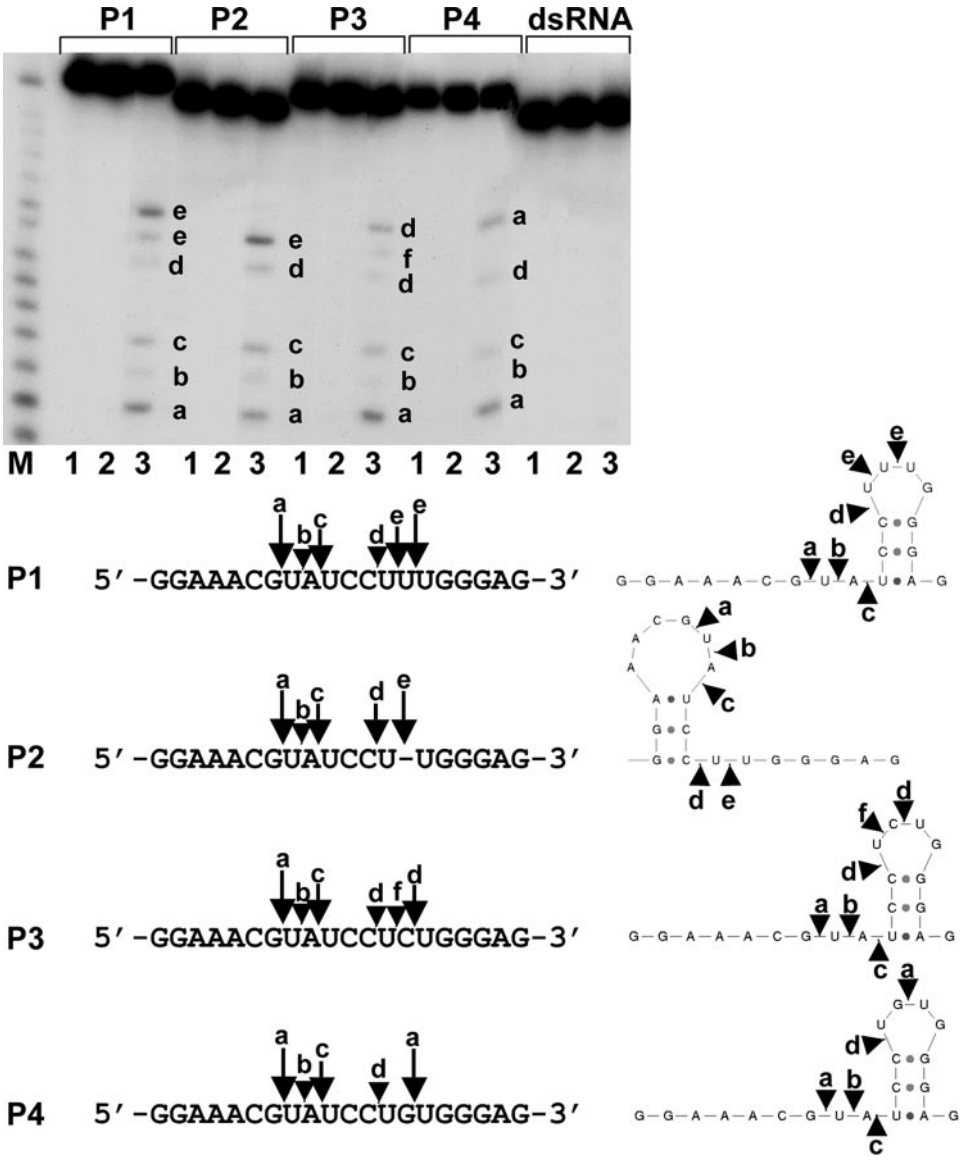

FIGURE 4. **Analysis of PP11 RNase activity.** *Top*, sequence specificity of His-PP11 cleavage activity was assessed by incubating, under standard conditions, P1, P2, P3, and P4 ^{32}P-labeled oligoribonucleotides (indicated *above* the gel) in the exclusive presence of Mn^{2+} ions (*lanes 2*) or by adding 100 ng of His-PP11 (*lanes 3*). Oligonucleotides were loaded as untreated molecules in *lanes 1*. His-PP11 RNase activity was also tested on P2 oligoribonucleotide in a double-stranded configuration (*lanes dsRNA*). In *lanes 1–3*, the RNA, treated as described for single stranded oligonucleotides, was loaded. In *lane M*, the nucleotide ladder, generated by alkaline digestion of the P1 oligonucleotide, was run as a molecular marker. *Bottom*, sequences of the synthetic oligoribonucleotides are reported. Reaction products were quantified by densitometric analysis, and cleavage sites are indicated by *arrows*. *Long arrows* indicate preferential His-PP11 cleavage sites, and *shorter arrows* point to sites processed less efficiently, whereas *arrowheads* refer to minor sites. *Letters* indicate sequence-specific cleavage sites (GU (*a*), UA (*b*), AU (*c*), CU (*d*), UU (*e*), and UC (*f*)) and are also reported for the corresponding reaction products on the gel. Oligoribonucleotide-predicted secondary structures, obtained by mfold software, are depicted on the *right*; cleavage sites are indicated by *arrowheads* and *letters*.

Identification of Residues Involved in Ribonuclease Activity—To define the residues participating in the enzymatic activity, we undertook a site-directed mutagenesis analysis. For this aim, we first probed the role of three residues, two histidines and a lysine that are highly conserved in proteins of the XendoU family (His^{162}, His^{178}, and Lys^{224} in XendoU) and that were implicated in XendoU and Nsp15 catalytic activities (8, 12, 13); their replacement was not tolerated either in coronavirus (13) or in *X. laevis* enzymes (12). We also tested two additional glutamic acid residues that were indispensable for XendoU activity (Glu^{161} and Glu^{167} in XendoU).

The following collection of His-PP11 mutant derivatives was produced. Two Glu residues, Glu^{243} and Glu^{249}, were substituted by Gln, giving rise to the single mutants E243Q and E249Q; substitution of His^{244} and His^{259} by Ala produced the mutants H244A and H259A, respectively. Finally, Lys^{302} was replaced by Ala, producing mutant K302A. The position of mutated residues in the PP11 homology model is reported in Fig. 2.

His-PP11 mutant derivatives were expressed as recombinant proteins in bacterial cells and, as a preliminary step for standardization of the following processing experiments, the protein amount needed to bind a constant quantity of RNA was established. For this aim, a fixed quantity (20 ng) of the single proteins were incubated with ^{32}P-labeled mini 003 RNA substrate, and the percentage of shifted RNA was evaluated in a mobility shift assay. As shown in the histogram of Fig. 6*A*, we found that the wild type as well as almost all the mutant proteins were able to shift a comparable percentage of the input RNA (about 20%), displaying the same efficiency in RNA binding activity, with E243Q protein showing a higher affinity.

Based on these evaluations, specific amounts of wild type and mutant proteins, producing the same percentage of shifted RNA, were incubated with a constant amount of ^{32}P-labeled P1 oligoribonucleotide, and their processing activity was analyzed. As shown in Fig. 6*B*, the mutants did not show any significant processing activity, with the mutant K302A displaying a slight residual activity. Such results indicate that each of the five residues is required for cleavage.

DISCUSSION

The "XendoU family" was proposed after the identification of several conserved viral proteins and was defined as a group of polypeptides with features as different as nucleases and proteases (8, 9). The best characterized members, XendoU (11) and Nsp15 (13), were defined as endoribonucleases playing a specific role in small RNA biogenesis in *Xenopus laevis* (10, 11, 25) and in

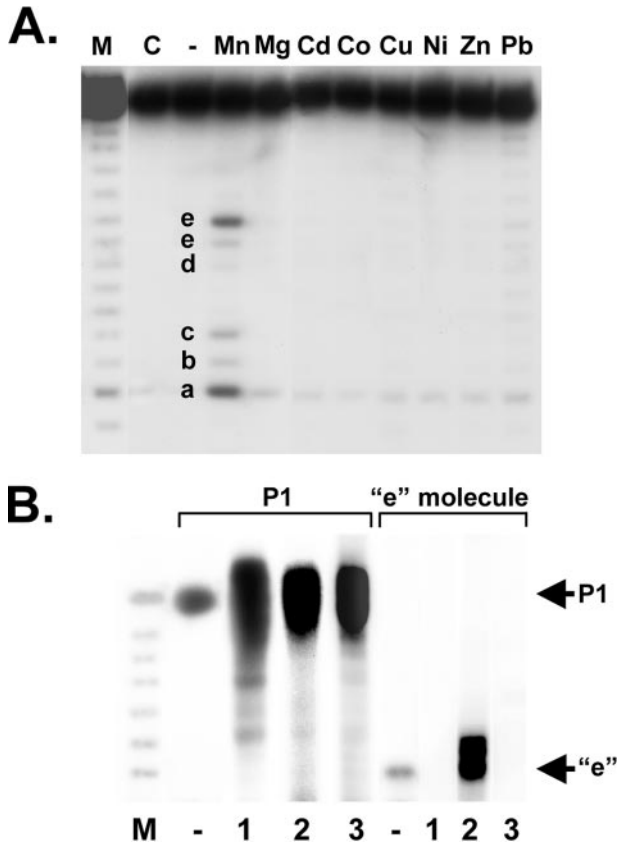

FIGURE 5. **Characterization of PP11 biochemical properties.** *A*, ion dependence of PP11 was defined by incubating ^{32}P-labeled P1 oligoribonucleotide (loaded as control in *lane C*) with the His-PP11 without ions (*lane −*) or in the presence of different cations (as indicated *above* each *lane*). The RNA ladder was fractionated in *lane M*. *Letters* indicating specific reaction products (see the legend to Fig. 4 for details) are reported on the gel. *B*, to determine the chemical nature of His-PP11 cleavage products, the more abundant "e" molecule (corresponding to the major "e" band in *A*), derived from the processing reaction of unlabeled P1 oligoribonucleotide, was treated with alkaline phosphatase (*lane 1*) or with kinase (*lane 2*) or with buffer alone (*lane 3*) and then labeled by 5′- [^{32}P]pCp and RNA ligase. Only after specific kinase treatment, removing the 2′,3′-cyclic phosphate, linear "e" molecules get labeled at their 3′-end. Full-length P1 substrate, bearing a linear 3′ terminus, was employed as a positive control; such a molecule was treated and analyzed as the "e" product. In *lanes −*, labeled "e" and P1 molecules were loaded as markers. The radiolabeled species are indicated by *arrows* on the *right*. The RNA ladder was fractionated in *lane M*.

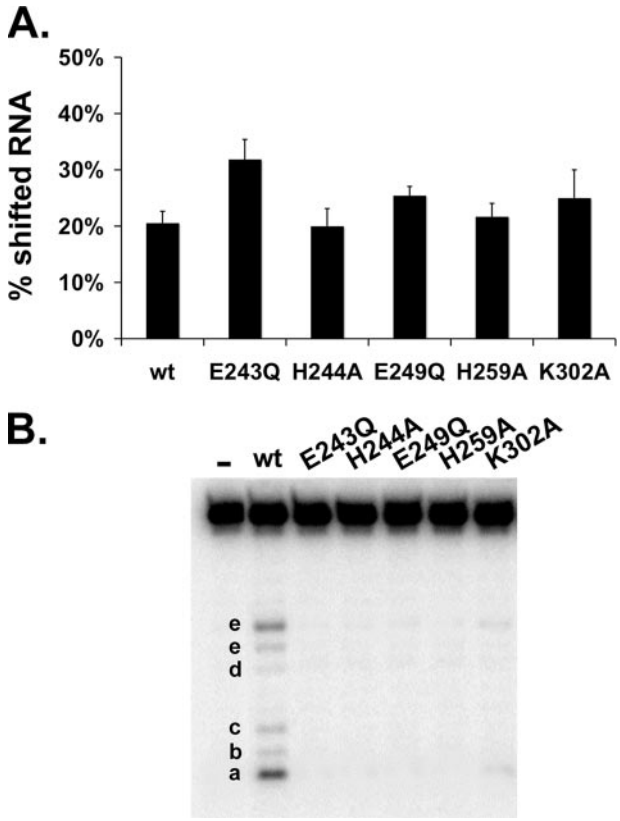

FIGURE 6. **Binding and processing activity of His-PP11 mutant derivatives.** *A*, the histogram reports the percentage of shifted RNA obtained by incubating, under standard binding conditions, mini 003 RNA substrate with 20 ng of wild type (*wt*) His-PP11or mutant derivatives thereof (indicated *below* each *bar*). *B*, amounts of wild type His-PP11 (*lane wt*) or of its mutant derivatives giving the same shift percentage of the RNA substrate (100 ng for each protein and 60 ng for E243Q) were employed in processing reactions on P1 oligoribonucleotide. Protein mutants are indicated *above* each *lane*. *Letters* indicating specific reaction products are reported on the gel; untreated substrate is loaded in *lane −*.

the coronavirus replication cycle (13), respectively. However, XendoU homologs from distantly related organisms were instead annotated as putative serine proteases on the basis of their homology with PP11 (human placental protein 11), described to have such an enzymatic activity (6). Subsequent phylogenetic alignment and secondary structure prediction of protein family members, together with crystallographic determination of XendoU structure (9), highlighted the occurrence of a conserved region that can be arranged in a common architecture, which is crucial for XendoU endoribonucleolytic activity.

These data prompted us to reconsider the biochemical nature of the putative serine proteases belonging to the same family. We focused on human PP11 and started with a homology modeling, based on XendoU tridimensional structural data (9). Our results revealed, in a conserved loop spanning from residue Gly^{248} to Asn^{260} (corresponding to Gly^{166}–Asn^{179} in XendoU), a specific site characterized by high flexibility that, as underscored by oligoribonucleotide docking experiments, may represent a RNA binding site.

To verify the ability of PP11 to bind and, possibly, to cleave RNA molecules, we undertook its biochemical characterization. Our data indicate the absence of protease activity in the recombinant His-PP11 that, instead, behaves as a Mn^{2+}-dependent, U-specific endoribonuclease. In this regard, we can suppose that the previously reported proteolytic activity, observed in the placental and in *E. coli* expressed proteins, was the result of contaminating activities originating from incomplete purification.

Overall, our results indicated that PP11 shares several biochemical features with the *Xenopus* and viral homologs: (i) they cleave RNA at uridylates, (ii) their activities are stimulated by Mn^{2+} ions, and (iii) they release 2′,3′-cyclic phosphodiester ends.

Altogether, these characteristics provide biochemical evidence for considering human PP11 as part of the XendoU family, not only on the basis of sequence homology but also in terms of enzymatic activity.

The functional parallel between PP11 and XendoU was further explored by defining the amino acid residues relevant for His-PP11 catalysis. Site-directed mutagenesis allowed the identification of two histidines, two glutamic acids, and a lysine that

are essential for RNA processing. Notably, all of them are included in the region that is highly conserved among all of the members of the XendoU family and that contains the residues involved in XendoU and Nsp15 catalytic activity (9). These data support the existence of a common domain, possibly shared by all the family members, that carries out a conserved RNA processing function. Comparative analysis of the PP11 structural model underscores the presence in the predicted RNA binding site of a loop more flexible than that of XendoU; this characteristic may account for the observed higher RNA affinity of PP11 and for its slightly different cleavage specificity.

Although the general enzymatic activity seems well defined for this class of proteins, more complicated is the definition of the variety of physiological functions in which they could participate. XendoU was previously described to be involved in the nuclear biosynthesis of small noncoding RNAs in *X. laevis*, whereas Nsp15 was defined to be essential for replication and transcription of human coronaviruses, responsible for respiratory disease, such as the common cold and severe acute respiratory syndrome (8). PP11 was isolated thanks to its high levels of expression in the syncitiotrophoblast and in several tumors, suggesting that in these cells, its function may be utilized for specialized/aberrant activities.

The syncytiotrophoblast is a placental tissue that derives from syncytial fusion of cytotrophoblast layers; the syncytialization involves the apoptotic cascade, and, as a consequence, fetal DNA and RNA can be detected in maternal blood (26). With regard to this very important process, PP11 could participate in cleavage followed by RNA degradation during the final stage of the apoptosis cascade (27). The RNase PP11 may also have a role in promoting tissue remodeling, a substantial feature of the trophoblast during all stages of pregnancy (28).

Since it has been postulated that the villous syncytiotrophoblast limits the transplacental transmission of viral pathogens (29), a further function can be postulated for PP11; through its RNA binding activity, it could recognize viral RNA genomes or mRNAs and trigger their degradation, participating in the defense mechanisms that preserve the fetus from viral infections during pregnancy. Detection of PP11 in several malignant cells (3–5) can instead suggest that its deregulated expression may be associated with oncogenesis. In this regard, we find intriguing the parallel between the physiological expression of PP11 in syncytiotrophoblastic cells and its aberrant expression in tumoral cells; both cell types are characterized by the capacity to invade the adjacent tissues.

In conclusion, our data assign a new enzymatic function to a previously characterized protein; we demonstrated that PP11 does not have protease activity, whereas it displays RNA binding and hydrolytic activities. Furthermore, the correspondence of the XendoU/PP11 amino acid residues participating in RNase function and the localization, by docking experiments, of the preferred PP11 cleavage dinucleotides into the corresponding XendoU phosphate binding region (9) highlights the evolutionary conservation of the catalytic/RNA binding site. Such conclusions, while opening new avenues of exploring PP11 biological roles, as well as the function of its homologs, through the identification of specific RNA substrates and binding partners, offer the chance to reconsider these proteins as important players in RNA metabolism.

Acknowledgments—We thank F. Palombi for helpful discussion and for advice in preparing cryosections, B. Muciaccia for expert assistance in immunofluorescent studies, and M. Marchioni for technical support. We also thank the medical and obstetrics staff of Clinica Ostetrica of "Sapienza" University of Rome for making available normal term placentas.

REFERENCES

1. Bohn, H., and Winckler, W. (1980) *Arch. Gynecol.* **229,** 293–301
2. Bohn, H., Inaba, N., and Luben, G. (1981) *Oncodev. Biol. Med.* **2,** 141–153
3. Inaba, N., Ishige, H., Ijichi, M., Satoh, N., Ohkawa, R., Sekiya, S., Shirotake, S., Takamizawa, H., Renk, T., and Bohn, H. (1982) *Oncodev. Biol. Med.* **3,** 379–389
4. Inaba, N., Renk, T., Daume, E., and Bohn, H. (1981) *Arch. Gynecol.* **231,** 87–90
5. Inaba, N., Renk, T., Wurster, K., Rapp, W., and Bohn, H. (1980) *Klin. Wochenschr.* **58,** 789–791
6. Grundmann, U., Romisch, J., Siebold, B., Bohn, H., and Amann, E. (1990) *DNA Cell Biol.* **9,** 243–250
7. Inaba, N., Renk, E., and Bohn, H. (1980) *Arch. Gynecol.* **230,** 109–121
8. Snijder, E. J., Bredenbeek, P. J., Dobbe, J. C., Thiel, V., Ziebuhr, J., Poon, L. L. M., Rozanov, Y. G. M., Spaan, W. J. M., and Gorbalenya, A. E. (2003) *J. Mol. Biol.* **331,** 991–1004
9. Renzi, F., Caffarelli, E., Laneve, P., Bozzoni, I., Brunori, M., and Vallone, B. (2006) *Proc. Natl. Acad. Sci. U. S. A.* **103,** 12365–12370
10. Caffarelli, E., Arese, M., Santoro, B., Fragapane, P., and Bozzoni, I. (1994) *Mol. Cell. Biol.* **14,** 2966–2974
11. Laneve, P., Altieri, F., Fiori, M. E., Scaloni, A., Bozzoni, I., and Caffarelli, E. (2003) *J. Biol. Chem.* **278,** 13026–13032
12. Gioia, U., Laneve, P., Dlakic, M., Arceci, M., Bozzoni, I., and Caffarelli, E. (2005) *J. Biol. Chem.* **280,** 18996–19002
13. Ivanov, K. A., Hertzig, T., Rozanov, M., Bayer, S., Thiel, V., Gorbalenya, A. E., and Ziebuhr, J. (2004) *Proc. Natl. Acad. Sci. U. S. A.* **101,** 12694–12699
14. Bhardwaj, K., Sun, J., Holzenburg, A., Guarino, L., and Kao, C. C. (2006) *J. Mol. Biol.* **361,** 243–256
15. Krisch, K. (1966) *Biochim. Biophys. Acta* **122,** 265–280
16. Renzi, F., Panetta, G., Vallone, B., Brunori, M., Arceci, M., Bozzoni, I., Laneve, P., and Caffarelli, E. (2006) *Acta Crystallogr. Sect. F* **62,** 298–301
17. Melton, D. A., Krieg, P. A., Rebagliati, M. R., Maniatis, T., Zinn, K., and Green, M. R. (1984) *Nucleic Acids Res.* **12,** 7035–7056
18. Pan, T., and Uhlenbeck, O. C. (1992) *Biochemistry* **31,** 3887–3895
19. Zuker, M. (2003) *Nucleic Acids Res.* **31,** 3406–3415
20. Roberts, S. A., and Ramsden, D. A. (2007) *J. Biol. Chem.* **282,** 10605–10613
21. Schwede, T., Kopp, J., Guex, N., and Peitsch, M. C. (2003) *Nucleic Acids Res.* **31,** 3381–3385
22. Soding, J., Biegert, A., and Lupas, A. N. (2005) *Nucleic Acids Res.* **33,** W244–W248
23. Morris, G. M., Goodsell, D. S., Halliday, R. S., Huey, R., Hart, W. E., Belew, R. K., and Olson, A. J. (1998) *J. Comput. Chem.* **19,** 1639–1662
24. Pinard, R., Lambert, D., Walter, N. G., Heckman, J. E., Major, F., and Burke, J. M. (1999) *Biochemistry* **38,** 16035–16039
25. Filippini, D., Renzi, F., Bozzoni, I., and Caffarelli, E. (2001) *Biochem. Biophys. Res. Commun.* **288,** 16–21
26. Gupta, A. K., Holzgreve, W., Huppartz, B., Malek, A., Schneider, H., and Hahn, S. (2004) *Clin. Chem.* **50,** 2187–2190
27. Huppertz, B., Frank, H. G., Kingdom, J. C., Reister, F., and Kaufmann, P. (1998) *Histochem. Cell Biol.* **110,** 495–508
28. Straszewski-Chavez, S. L., Abrahams, V. M., and Mor, G. (2005) *Endocr. Rev.* **26,** 877–897
29. Koi, H., Zhang, J., Makrigiannakis, A., Getsios, S., Maccalman, C. D., Kopf, G. S., Strauss, J. F., III, and Parry, S. (2000) *BIOONE Online J.* **64,** 1001–1009